Journal of Materials Chemistry C

PAPER

View Article Online
View Journal | View Issue

Published on 21 August 2014. Downloaded by University of Western Ontario on 28/10/2014 14:34:46.

Cite this: J. Mater. Chem. C, 2014, 2, 8515

Property modulation of benzodithiophene-based polymers *via* the incorporation of a covalently bonded novel 2,1,3-benzothiadiazole-1,2,4-oxadiazole derivative in their main chain for polymer solar cells

Rajalingam Agneeswari,[a] Vellaiappillai Tamilavan,[a] Myungkwan Song*[b] and Myung Ho Hyun*[a]

Received 17th July 2014
Accepted 19th August 2014

DOI: 10.1039/c4tc01558d

www.rsc.org/MaterialsC

Two new electron accepting monomers (**BBOB** and **BOB**) containing two serially connected different electron deficient units, such as 2,1,3-benzothiadiazole and 1,2,4-oxadiazole, were prepared and copolymerized with electron-rich benzodithiophene (**BDT**) derivative to afford polymers **P(BDT-BBOB)** and **P(BDT-BOB)**, respectively. The optical band gaps of **P(BDT-BBOB)** and **P(BDT-BOB)** are calculated to be 2.32 eV and 1.99 eV, respectively, and their highest occupied molecular energy levels are determined to be −5.31 eV and −5.27 eV, respectively. Each of the newly synthesized polymers, *i.e.* **P(BDT-BBOB)** and **P(BDT-BOB)**, is used as an electron donor, along with $PC_{61}BM$ as an electron acceptor, in the preparation of polymer solar cells (PSCs). The PSCs made with the configuration of ITO/PEDOT:PSS/**P(BDT-BBOB)** or **P(BDT-BOB)**:$PC_{61}BM$ (1 : 2 wt%)/LiF/Al gave a maximum power conversion efficiency (PCE) of 1.76% and 2.46%, respectively, and the device performance was further improved to 3.31% and 4.21%, respectively, by simply treating the photoactive layer of PSCs with isopropyl alcohol. Overall, the opto-electrical and photovoltaic properties of the two polymers are found to be quite dependent on the configuration of the covalently bonded 2,1,3-benzothiadiazole and 1,2,4-oxadiazole units incorporated in the polymer main chain.

1. Introduction

Recent progress in polymer solar cells (PSCs) demonstrates that they are promising renewable energy production techniques, due to their advantages, such as flexible and light weight device fabrication at low cost *via* standard roll-to-roll (R2R) printing techniques.[1] The maximum solar to electrical energy conversion efficiency (PCE) of PSCs made from the blends of an electron donating π-conjugated polymer and an electron accepting fullerene derivative (such as $PC_{61}BM$, $PC_{71}BM$ or ICBM) is improved in the range of 9–10.5% with the use of tandem structured PSCs,[2–7] while a PCE in the range of 7–9% is obtained for single layer PSCs.[8–13] Only one type of polymer (either low or large band gap) is used in the photoactive layer of single layer PSCs,[8–13] while both large and low band gap polymers are used in tandem PSCs, to utilize the entire energy in the visible-NIR part of the solar spectra, and consequently, tandem PSCs have a higher PCE than single layer PSCs.[2–7] The theoretical studies suggest that the maximum PCE of single layer PSCs could reach up to 17% and that tandem PSCs have the capability for a maximum PCE of 24%.[14]

It is essential to develop structurally novel polymers showing better opto-electrical and photovoltaic properties than the known polymers to boost the PSC performances further. The literature reveals that polymers incorporating electron deficient 2,1,3-benzothiadiazole (BT),[9] thieno[3,4-*b*]-thiophene (TT),[10] thieno[3,4-*c*]pyrrole-4,6-dione (TPD),[11] and pyrrolo[3,4-*c*]pyrrole-1,4-dione (DKPP)[12,13] derivatives show excellent absorption, and high carrier mobility, and consequently high PCE in both single and tandem PSCs.[2–13] Among these, the BT analogue is considered as the most promising acceptor unit, and polymers incorporating a BT unit gave a maximum PCE of 8.2% and 10.6%, respectively, in single layer and tandem PSCs.[6,9]

Dennler *et al.* discussed about the importance of tuning the HOMO and LUMO energy levels of the alternating donor–acceptor (D–A) polymers *via* the modification of the donor or acceptor unit in the polymer main chain to maximize the device efficiency of single or tandem PSCs. They also clearly

[a]Department of Chemistry, Chemistry Institute for Functional Materials, Pusan National University, Busan 690-735, Republic of Korea. E-mail: mhhyun@pusan.ac.kr; Fax: +82-51-516-7421; Tel: +82-51-510-2245

[b]Surface Technology Division, Korea Institute of Materials Science (KIMS), Changwon, Gyeongnam 641-831, Republic of Korea. E-mail: smk1017@kims.re.kr; Fax: +82-55-280-3570; Tel: +82-55-280-3686

Published on 21 August 2014. Downloaded by University of Western Ontario on 28/10/2014 14:34:46.

demonstrated that the PCE of the PSCs is related to the band gap and HOMO–LUMO energy levels of the donor martial.[8] Consequently, many studies have shown that the photovoltaic properties of the polymers incorporating BT-based acceptor units can be tuned *via* the incorporation/insertion of electron donating or accepting units on the BT moiety.[15–28] In most of the studies, electron donating units,[15–21] such as benzene, thiophene, thienothiophene, and furan derivatives, are covalently attached on both sides of the BT unit or electron-rich alkoxy,[20,21] or electron-attracting fluorides[8,28] are inserted on the back bone of the BT unit with the aim being to improve the absorption and carrier mobility and to tune the energy levels of the BT-based polymers. In addition, electron accepting units, such as thiazole[22] and benzimidazole,[23] are also attached on both sides of the BT units or quinoxaline,[24,25] and thiadiazole[26] and *N*-alkylpyrrolidine-2,5-dione rings[27] are fused on the BT back bone with the aim being to increase the electron attracting ability of the BT unit. Some examples of BT-based acceptor units are presented in Fig. 1. Recently, we reported a series of 1,2,4-oxadiazole (Oxa)-based polymers for PSC applications.[29] Polymers incorporating separate BT and Oxa units in the polymer main chain were found to show broad absorption in the range 300–900 nm.[29] However, polymers incorporating covalently bonded BT-Oxa units have not yet been reported. We believe that the covalent attachment of the high electron transporting Oxa unit on the BT unit increases the electron deficiency, as well as improves the electron mobility. Consequently, when the BT-Oxa unit is polymerized with electron-rich units, broad absorbing polymers with high electron mobility are expected. In order to clearly understand the opto-electrical and photovoltaic properties of polymers incorporating the covalently bonded BT-Oxa unit, we prepared two different electron deficient monomers, namely, **BBOB** (Oxa-BT-Oxa derivative) and **BOB** (BT-Oxa derivative). The strong electron deficient monomers, such as **BBOB** and **BOB**, were copolymerized with a distannyl derivative of 4,8-bis(2-ethylhexyloxy)benzo[1,2-*b*:4,5-*b*′]-dithiophene (**BDT**), to give polymers **P(BDT-BBOB)** and **P(BDT-BBOB)**, respectively. In this study, we report the synthesis, optical, electrochemical and photovoltaic properties of the two new polymers, **P(BDT-BBOB)** and **P(BDT-BBOB)**, incorporating covalently bonded BT-Oxa units in their main chain.

2. Experimental section

2.1 Materials and instruments

The reagents were received from Aldrich or TCI chemicals and used without further purification. The common organic solvents were distilled and handled in a moisture-free atmosphere. The column purification of the compounds was performed on silica gel (Merck Kieselgel 60, 70–230 mesh ASTM). The compounds were characterized by using nuclear magnetic resonance (NMR) spectra performed on a Varian Mercury Plus spectrometer (300 MHz and 75 MHz, respectively, for ^{1}H and ^{13}C) and high resolution mass spectra performed on a JEOL JMS700 mass spectrometer. The molecular weights of the polymers were determined from gel permeation chromatography (GPC) analyses by using an Agilent 1200 Infinity Series separation module using polystyrene as a standard and chloroform as an eluent. Thermogravimetric analyses (TGA) were conducted with a TA instrument Q500 at a heating rate of 10 °C min^{-1} under nitrogen. The absorption spectra of the polymers were recorded on a JASCO V-570 spectrophotometer at 25 °C in chloroform or as thin films on quartz. The cyclic voltammetry (CV) measurements were performed on a CH Instruments Electrochemical Analyzer. Electrochemical measurements were performed with polymer cast platinum as a working electrode, Ag/AgCl as a reference electrode, and platinum wire as a counter electrode in 0.1 M tetrabutylammonium tetrafluoroborate (Bu_4NBF_4) acetonitrile solution. The impedance responses of polymer:$PC_{61}BM$ blends were measured over the range from 1 Hz to 1 MHz with an oscillation amplitude of 15 mV (Bio-Logic VMP-3). The experimental data were simulated using commercial Z-view software to estimate the values for each component of the corresponding equivalent circuits.

2.2 Fabrication and characterization of PSCs

The device fabrication and characterization of PSCs are summarized below. Indium tin oxide (ITO)-coated glass substrates were cleaned stepwise by acetone, deionized water, and isopropyl alcohol in an ultrasonic bath. Then a 50 nm poly(ethylenedioxythiophene)-poly(styrenesulfonate) (PEDOT:PSS) (Clevious P: isopropyl alcohol, 1 : 2 v/v%) buffer layer was spin-coated on the top of the ITO substrate at 5000 rpm for 40 s and dried at 150 °C for 10 min under vacuum to remove the residual water. The active layer of the polymer and $PC_{61}BM$

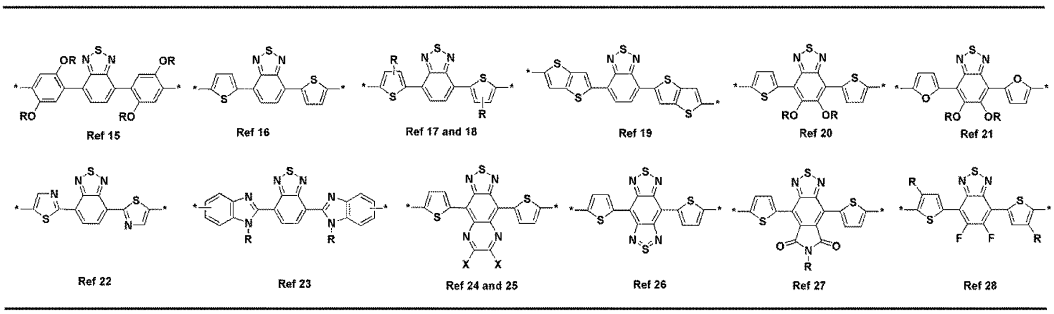

Fig. 1 Few examples of 2,1,3-benzothiadiazole (BT)-based acceptor units.

 This journal is © The Royal Society of Chemistry 2014

Published on 21 August 2014. Downloaded by University of Western Ontario on 28/10/2014 14:34:46.

blend (1 : 1 wt%, 1 : 2 wt%, and 1 : 3 wt%) was spin-coated at 800 rpm from dichlorobenzene (DCB) solution on the top of the ITO/PEDOT:PSS substrate. The ITO/PEDOT:PSS/polymer:$PC_{61}BM$ substrate was allowed to dry for 10 min in a glove box and then subjected to pre-annealing at 80 °C for 10 min. The thickness of the photoactive layer was found to be around 80 nm. Isopropyl alcohol (IPA) was spin-coated on the top of the ITO/PEDOT:PSS/polymer:$PC_{61}BM$ substrate at 3000 rpm for 40 s for the devices subjected to solvent treatments, and then ~0.7 nm thick layer of LiF was deposited on the substrate. Subsequently, a 100 nm thick layer of Al was deposited through a shadow mask on the top of the ITO/PEDOT:PSS/polymer:$PC_{71}BM$/LiF substrate under a high vacuum (1.2×10^{-6} torr). The top metal electrode area, comprising the active area of the solar cell, was found to be 0.36 cm^2. The *J–V* characteristics of the devices were measured using a Keithley 2400 source measure unit under a calibrated AM 1.5G solar simulator (Oriel® Sol3A™ Class AAA solar simulator, models 94043A) at 100 mW cm^{-2}. The intensity of the sunlight illumination was calibrated using a standard Si photodiode detector with a KG-5 filter. The IPCE measurement system (Oriel IQE-200) was composed of a 250 W quartz–tungsten–halogen (QTH) lamp as the light source, as well as a monochromator, optical chopper, lock-in amplifier, and calibrated silicon photodetector.

2.3 Synthesis of monomers

Benzo[*c*][1,2,5]thiadiazole-4,7-dicarbonitrile (1). To a stirred solution of 4,7-dibromobenzo[*c*][1,2,5]thiadiazole (7.35 g, 25 mmol) in *N*,*N*-dimethylformamide (DMF, 70 mL) was added copper cyanide (9.0 g, 100 mmol). The mixture was heated to 150 °C for 72 h and then it was cooled to room temperature (RT). The mixture was poured into 2 N HCl (200 mL) and extracted (2 × 100 mL) with ethyl acetate (EA). The combined organic layer was washed well with brine solution and then the organic layer was dried over anhydrous Na_2SO_4. The solvent was removed by rotary evaporation and the crude product was purified by column chromatography (silica gel, hexane:CH_2Cl_2, 20/80) to afford compound **1** as a colorless solid. Yield: 2.2 g (47%). ^{1}H NMR (300 MHz, $CDCl_3$): δ (ppm) 8.15 (s, 2H); ^{13}C NMR (75 MHz, $CDCl_3$): δ (ppm) 152.6, 134.7, 114.1, 110.9; HRMS (EI^+, *m*/*z*) [M^+] calcd for $C_8H_2N_4S$ 186.0000, found 186.0006.

(4*Z*,7*Z*)-*N*4′,*N*7′-Dihydroxybenzo[*c*][1,2,5]thiadiazole-4,7-dicarboxamidine (2). To a stirred solution of compound **1** (1.0 g, 5.40 mmol) in chloroform (10 mL) was added ethanol (60 mL) and 50% aqueous hydroxylamine solution (10 mL). Then, the whole mixture was heated to reflux for 3 h. The completion of the reaction was confirmed by TLC, and ethanol was removed by rotary evaporation. The crude product was washed with cold ethanol, diethyl ether and hexane. The solid was dried under vacuum to afford compound **2** as a yellow colored solid. Yield: 1.1 g (81%). ^{1}H NMR (300 MHz, DMSO-d_6): δ (ppm) 10.00 (s, 2H), 7.99 (s, 2H), 6.24 (s, 4H).

4,7-Bis(5-(4-bromo-2,5-bis(octyloxy)phenyl)-1,2,4-oxadiazol-3-yl)benzo[*c*][1,2,5]thiadiazole (BBOB). To a stirred solution of compound **3** (0.50 g, 1.10 mmol), which was prepared by the reported procedure,[30] in DMF (5 mL) was added 1,1′-carbonyldiimidazole (CDI, 0.19 g, 1.20 mmol), followed by stirred for 30 min. Then, (4*Z*,7*Z*)-*N*4′,*N*7′-dihydroxybenzo[*c*]-[1,2,5]thiadiazole-4,7-dicarboxamidine (**2**) (0.13 g, 0.50 mmol) in DMF (10 mL) was added dropwise to the stirred solution. The solution was stirred overnight and then poured into water. The aqueous layer was extracted (3 × 30 mL) with chloroform ($CHCl_3$). The combined organic layer was dried over anhydrous Na_2SO_4. The solvent was removed by rotary evaporation and the resulting sticky mass was dissolved in anhydrous toluene (30 mL). The solution was refluxed for 24 h and then toluene was removed by rotary evaporation. The crude product was purified by column chromatography (silica gel, CH_2Cl_2) to afford **BBOB** as a yellow colored solid. Yield: 0.32 g (58%). ^{1}H NMR (300 MHz, $CDCl_3$): δ (ppm) 8.74 (s, 2H), 7.73 (s, 2H), 7.32 (s, 2H), 4.10 (q, 8H), 1.80–2.00 (m, 8H), 1.40–1.60 (m, 8H), 1.10–1.40 (m, 32H), 0.80–1.10 (m, 12H); ^{13}C NMR (75 MHz, $CDCl_3$): δ (ppm) 175.0, 165.8, 152.9, 152.3, 150.0, 130.9, 122.9, 119.3, 115.2, 112.7, 70.5, 70.4, 32.1, 32.0, 29.6, 29.5, 29.4, 26.2, 22.9, 14.3; HRMS (EI^+, *m*/*z*) [M^+] calcd for $C_{54}H_{74}Br_2N_6O_6S$ 1092.3757, found 1092.3750.

3-Methylbenzene-1,2-diamine (4). According to the reported procedure, the nitro group on 3-methyl-2-nitrobenzenamine was reduced to an amino group by using $SnCl_2$ to afford compound **4**.[31] However, in this study, the nitro to amino group conversion was performed by using palladium/carbon. The modified procedure decreases the reaction time and gives a high yield compared to the reported procedure. To a stirred solution of 3-methyl-2-nitrobenzenamine (5.0 g, 33.0 mmol) in methanol (200 mL) was added 0.75 g of palladium on carbon (10 wt% loading, matrix carbon, dry support) and ammonium formate (15.5 g, 165 mmol). Then, the mixture was heated to 70 °C for 3 h. The completion of the reaction was confirmed by TLC, and the palladium on carbon was filtered out. The solvent was removed and the resulting solid material was dissolved in EA (100 mL). The organic solution was washed once with aqueous 2 N sodium hydroxide solution and then the organic layer was dried over anhydrous Na_2SO_4. The solvent was removed by rotary evaporation and the product was dried under vacuum to afford compound **4** as a brown colored solid. Yield: 3.94 g (98%). ^{1}H NMR (300 MHz, $CDCl_3$): δ (ppm) 6.60–6.70 (m, 3H), 3.38 (s, 4H), 2.20 (s, 3H); ^{13}C NMR (75 MHz, $CDCl_3$): δ (ppm) 134.1, 133.7, 123.6, 122.3, 119.4, 115.3, 17.71.

4-Methylbenzo[*c*][1,2,5]thiadiazole (5). The synthetic procedure for compound **5** was already reported,[31] but, in this study, we developed a slightly modified, more efficient and facile procedure. A stirred solution of compound **4** (3.7 g, 30.3 mmol) in dry CH_2Cl_2 (150 mL) was cooled to 0 °C in an ice bath for 15 min and then triethyl amine (17 mL, 121 mmol) was slowly added. Then, thionyl chloride (4.4 mL, 60.6 mmol) in dry CH_2Cl_2 (50 mL) was added dropwise at 0 °C. After the addition, the solution was allowed to stir for 1 h and then heated to 40 °C for 15 h. The reaction mixture was cooled to RT and poured into 2 N HCl (200 mL) and the organic layer was then separated. The organic layer was dried over anhydrous Na_2SO_4. The crude product was purified by column chromatography (silica gel, hexane:EA, 80/20) to afford compound **5** as a brown colored liquid. Yield: 4.2 g (92%). ^{1}H NMR (300 MHz, $CDCl_3$): δ (ppm) 7.83 (1, 2H), 7.47 (t, 2H), 7.33 (d, 1H), 2.74 (s, 3H); ^{13}C NMR

Published on 21 August 2014. Downloaded by University of Western Ontario on 28/10/2014 14:34:46.

(75 MHz, $CDCl_3$): δ (ppm) 155.6, 155.2, 131.9, 129.8, 128.2, 119.2, 18.2.

4-Bromo-7-methylbenzo[*c*][1,2,5]thiadiazole (6). Compound **6** was prepared *via* the similar reported procedure.[31] Compound **5** (3.2 g, 21.3 mmol) and 48% HBr (80 mL) were stirred at RT. To this solution was added Br_2 (1.20 mL, 22 mmol) in 48% HBr (80 mL) dropwise. Then, the mixture was heated to reflux for 16 h. The solution was cooled to RT and the mixture was poured into saturated sodium bisulfite solution. The mixture was stirred for 30 min and then extracted (2 × 100 mL) with CH_2Cl_2. The combined organic layer was dried over anhydrous Na_2SO_4, filtered, and then the solvent was evaporated by rotary evaporation. The crude product was purified by column chromatography (silica, hexane:EA, 90/10) to afford compound **6** as a colorless solid. Yield: 4.5 g (92%). ^{1}H NMR (300 MHz, $CDCl_3$): δ (ppm) 7.72 (d, 1H), 7.22 (d, 1H), 2.70 (s, 3H); ^{13}C NMR (75 MHz, $CDCl_3$): δ (ppm) 155.4, 153.4, 132.3, 131.5, 129.1, 111.4, 17.9.

4-Bromo-7-(bromomethyl)benzo[*c*][1,2,5]thiadiazole (7). Compound **7** was prepared *via* the similar reported procedure.[31] Compound **6** (4.0 g, 17.4 mmol), *N*-bromosuccinimide (NBS, 3.1 g, 17.5 mmol) and benzoyl peroxide (10 mg) were dissolved in CCl_4 (140 mL). The solution was heated to reflux and 33% HBr in acetic acid (1 mL) was added. After 3 h, the reaction mixture was poured into water (100 mL). The organic layer was separated and dried over anhydrous Na_2SO_4, filtered, and then the solvent was evaporated by rotary evaporation. The crude product was purified by column chromatography (silica, hexane:EA, 90/10) to afford compound **7** as a colorless solid. Yield: 4.5 g (92%). ^{1}H NMR (300 MHz, $CDCl_3$): δ (ppm) 7.81 (d, 1H), 7.53 (d, 1H), 4.94 (s, 2H); ^{13}C NMR (75 MHz, $CDCl_3$): δ (ppm) 155.4, 153.4, 132.3, 131.5, 128.8, 114.5, 27.9.

7-Bromobenzo[*c*][1,2,5]thiadiazole-4-carbaldehyde (8). Compound **8** was prepared *via* the slightly modified procedure.[32] Compound **7** (2.8 g, 9.1 mmol) and sodium periodate ($NaIO_4$) (0.42 g, 2.3 mmol) were added in a round bottom flask and then DMF (30 mL) was added. The reaction mixture was heated at 150 °C for 3 h. Again, $NaIO_4$ (0.42 g, 2.3 mmol) was added to the solution with continuous stirring for 2 h at 150 °C. The reaction mixture was cooled and poured into water (100 mL) and then extracted with EA (2 × 50 mL). The combined organic layer was dried over anhydrous Na_2SO_4, filtered, and then the solvent was evaporated by rotary evaporation. The crude product was purified by column chromatography (silica, hexane:EA, 90/10) to afford compound **8** as a yellow colored solid. Yield: 1.2 g (54%). ^{1}H NMR (300 MHz, $CDCl_3$): δ (ppm) 10.73 (s, 1H), 8.11 (d, 1H), 8.06 (d, 1H); ^{13}C NMR (75 MHz, $CDCl_3$): δ (ppm) 188.6, 154.5, 152.6, 132.4, 132.0, 127.1, 122.2.

7-Bromobenzo[*c*][1,2,5]thiadiazole-4-carbonitrile (9). Compound **9** was prepared *via* a previously reported procedure.[33] A stirred solution of compound **8** (1.0 g, 4.1 mmol) and hydroxylamine hydrochloride (0.57 g, 8.2 mmol) in DMSO (30 mL) was heated at 100 °C for 2 h. Then, the reaction mixture was cooled to RT and poured into water (100 mL). The mixture was stirred for 30 min and then allowed to settle down. The precipitates were filtrated off and washed well with MeOH and hexane. The solid was dried under vacuum to afford compound **9** as a colorless solid. Yield: 0.82 g (84%). ^{1}H NMR (300 MHz, $CDCl_3$): δ (ppm) 7.96 (d, 2H), 7.91 (d, 2H); ^{13}C NMR (75 MHz, $CDCl_3$): δ (ppm) 153.3, 152.6, 136.1, 131.6, 121.5, 115.0, 105.6.

(*Z*)-7-Bromo-*N*′-hydroxybenzo[*c*][1,2,5]thiadiazole-4-carboxamidine (10). To a stirred solution of compound **9** (0.7 g, 2.9 mmol) in ethanol (60 mL) was added 50% aqueous hydroxylamine solution (10 mL). The mixture was heated to reflux for 3 h. The completion of the reaction was confirmed by TLC, and ethanol was removed by rotary evaporation. The crude product was washed with diethyl ether and hexane. The solid was dried under vacuum to afford compound **10** as a yellow colored solid. Yield: 0.65 g (82%). ^{1}H NMR (300 MHz, CD_3OD): δ (ppm) 7.97 (d, 2H), 7.86 (d, 2H), 3.25 (s, 1H).

4-Bromo-7-(5-(4-bromo-2,5-bis(octyloxy)phenyl)-1,2,4-oxadiazol-3-yl)benzo[*c*][1,2,5]thiadiazole (BOB). Under an argon atmosphere, to the solution of compound **3** (0.64 g, 1.4 mmol) in DMF (10 mL) was added 1,1′-carbonyldiimidazole (CDI, 0.23 g, 1.4 mmol). The whole mixture was stirred for 30 min. Then, compound **10** (0.38 g, 1.4 mmol) in DMF (10 mL) was added dropwise to the stirred solution. The solution was stirred overnight and then poured into water. The aqueous layer was extracted (3 × 30 mL) with chloroform ($CHCl_3$). The combined organic layer was dried over anhydrous Na_2SO_4. The solvent was removed by rotary evaporation and the resulting sticky mass was dissolved in anhydrous toluene (30 mL). The solution was refluxed for 24 h and then the toluene was removed by rotary evaporation. The crude product was purified by column chromatography (silica, hexane:EA, 80/20) to afford **BOB** as a yellow colored solid. Yield: 0.53 g (55%). ^{1}H NMR (300 MHz, $CDCl_3$): δ (ppm) 8.46 (d, 1H), 8.00 (d, 1H), 7.69 (s, 1H), 7.30 (s, 1H), 4.08 (q, 4H), 1.80–2.00 (m, 4H), 1.40–1.60 (m, 4H), 1.20–1.40 (m, 16H), 0.90–1.00 (m, 6H); ^{13}C NMR (75 MHz, $CDCl_3$): δ (ppm) 174.8, 165.7, 154.1, 152.9, 151.3, 150.0, 132.0, 131.7, 120.1, 119.3, 119.2, 118.2, 115.2, 112.7, 70.5, 70.4, 32.1, 32.0, 29.5, 29.4, 26.2, 22.9,14.3; HRMS (EI$^+$, *m*/*z*) [M$^+$] calcd for $C_{30}H_{38}Br_2N_4O_3S$ 692.1031, found 692.1036.

Poly(4,8-bis(2-ethylhexyloxy)benzo[1,2-*b*:4,5-*b*′]dithiophene-*alt*-4,7-bis(5-(2,5-bis(octyloxy)phenyl)-1,2,4-oxadiazol-3-yl)benzo[*c*][1,2,5]thiadiazole) (P(BDT-BBOB)). A solution of the respective monomers, such as **BDT** (0.23 g, 0.3 mmol) and **BBOB** (0.33 g, 0.3 mmol) in chlorobenzene (30 mL), was degassed well with argon for 45 min. Then, Pd_2dba_3 (0.14 g) and P(*o*-tol)$_3$ (0.30 g) were added. The stirred solution was heated to reflux under an argon atmosphere for 48 h. Then, the solution was dropwise added to the vigorously stirred methanol (200 mL). The precipitate was recovered by filtration, and then extracted with methanol for 24 h and acetone for 24 h in a Soxhlet apparatus to afford pure polymer **P(BDT-BBOB)** as a light brown colored solid. Yield: 0.37 g (90%). GPC (Chloroform): $M_n = 1.85 \times 10^4$ g mol^{-1}; $M_w = 1.28 \times 10^4$ g mol^{-1}; PDI = 1.45. Elemental analysis calcd for $(C_{80}H_{112}N_6O_8S_3)_n$: C, 69.53; H, 8.17; N, 6.08; S, 6.96. Found: C, 70.30; H, 7.86; N, 5.70; S, 7.01.

Poly(4,8-bis(2-ethylhexyloxy)benzo[1,2-*b*:4,5-*b*′]dithiophene-*alt*-4-(5-(2,5-bis(octyloxy)phenyl)-1,2,4-oxadiazol-3-yl)benzo[*c*]-[1,2,5]thiadiazole) (P(BDT-BOB)). For the preparation of **P(BDT-BOB)**, the synthetic procedure similar to that for the preparation of (**P(BDT-BBOB)**) was used. In this reaction, monomers **BDT** (0.23 g, 0.3 mmol) and **BOB** (0.21 g, 0.3 mmol) were used

 This journal is © The Royal Society of Chemistry 2014

Published on 21 August 2014. Downloaded by University of Western Ontario on 28/10/2014 14:34:46.

for the polymerization. Polymer (**P(BDT-BOB)**) was obtained as a dark brown colored solid. Yield: 0.26 g (90%). GPC (chloroform): $M_n = 2.13 \times 10^4$ g mol^{-1}; $M_w = 1.30 \times 10^4$ g mol^{-1}; PDI = 1.63. Elemental analysis calcd for $(C_{56}H_{76}N_4O_5S_3)_n$: C, 68.53; H, 7.81; N, 5.71; S, 9.80. Found: C, 66.95; H, 7.93; N, 4.74; S, 9.16.

3. Results and discussion

3.1 Synthesis and structural characterization

The synthetic route for the monomers (**BBOB** and **BOB**) and polymers (**P(BDT-BBOB)** and **P(BDT-BOB)**) are outlined in Scheme 1 and Scheme 2, respectively. Benzo[*c*][1,2,5]thiadiazole-4,7-dicarbonitrile (**1**) was prepared by treating 4,7-dibromobenzo[*c*][1,2,5]thiadiazole with copper cyanide. Compound **1** was converted into compound **2** by treating with 50% aqueous hydroxyl amine solution. On the other hand, compound **3** was prepared by using the reported procedure.[30] The acid group on compound **3** was activated by treating with coupling agent (CDI) and then reaction with compound **2**, followed by cyclization, to afford the monomer **BBOB** containing two Oxa units and one BT unit. Another monomer, namely, **BOB**, was prepared from 3-methyl-2-nitrobenzenamine. In this route, the nitro group on 3-methyl-2-nitrobenzenamine was reduced to the amino group with the use of Pd/C, to give compound **4**. Compound **4** was treated with thionyl chloride and TEA in dichloromethane to afford compound **5**. The bromination of compound **5** with bromine afforded compound **6**, and then compound **6** was treated with NBS to afford compound **7**.[31] The $NaIO_4$ oxidation[32] of compound **7** gave compound **8**, and the formyl group of compound **8** was converted to the cyano group of compound **9** by treating with hydroxyl amine hydrochloride ($NH_2OH \cdot HCl$).[33] Compound **10** and monomer **BOB** were prepared *via* the synthetic procedure used for the synthesis of compound **2** and **BBOB**, respectively. The ^{1}H and ^{13}C NMR spectra of **BBOB** and **BOB** are presented in Fig. 2.

The Stille polymerization between the most promising electron-rich **BDT** and the new electron-accepting **BBOB** and **BOB** afforded polymers **P(BDT-BBOB)** and **P(BDT-BOB)**, respectively. Both the polymers **P(BDT-BBOB)** and **P(BDT-BOB)** show good solubility in chloroform, chlorobenzene, and dichlorobenzene, and their weight average molecular weights (M_w) and polydispersities (PDI) determined by GPC analysis with chloroform as an eluent were 1.85×10^4, 2.13×10^4 and 1.45 and 1.63, respectively. The 5% weight loss temperatures of **P(BDT-BBOB)** and **P(BDT-BOB)** were found to be 407 °C and 415 °C, respectively, from thermogravimetric analysis (TGA). The good solubility and high thermal stability of **P(BDT-BBOB)** and **P(BDT-BOB)** allow them to be utilized in PSCs. The molecular weights and 5% weight loss temperatures of **P(BDT-BBOB)** and **P(BDT-BOB)** are summarized in Table 1.

3.2 Optical properties

The absorption spectra of the polymers **P(BDT-BBOB)** and **P(BDT-BOB)** measured in chloroform and as a thin film on glass are presented in Fig. 3. Polymer **P(BDT-BBOB)** displays an absorption band in the range of 300–520 nm, with two maximum absorption peaks at 399 and 454 nm in solution and 416 and 455 nm as a film. On the other hand, polymer **P(BDT-BOB)** showed a broad absorption band in between 300 nm and 600 nm, with maximum absorption peaks at 431 and 509 nm,

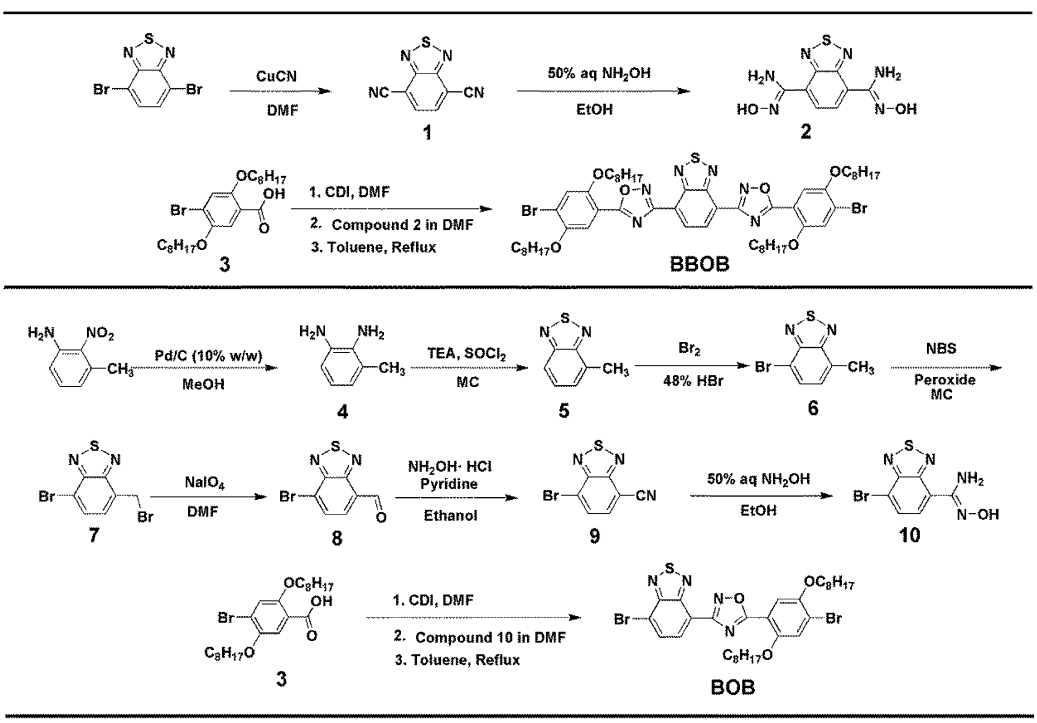

Scheme 1 Synthetic route to monomers BBOB and BOB.

Published on 21 August 2014. Downloaded by University of Western Ontario on 28/10/2014 14:34:46.

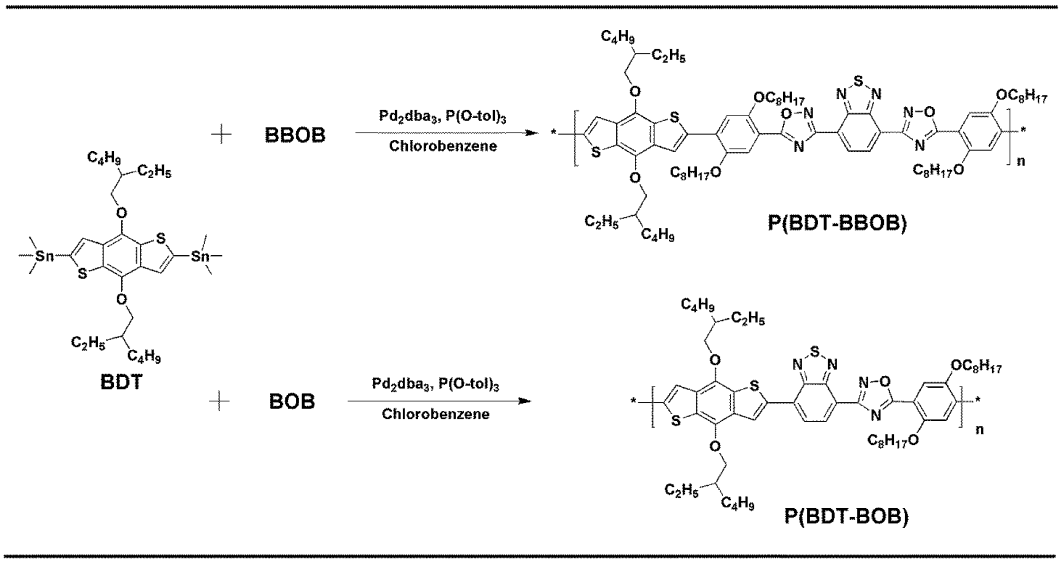

Scheme 2 Synthetic route to polymers P(BDT-BBOB) and P(BDT-BOB).

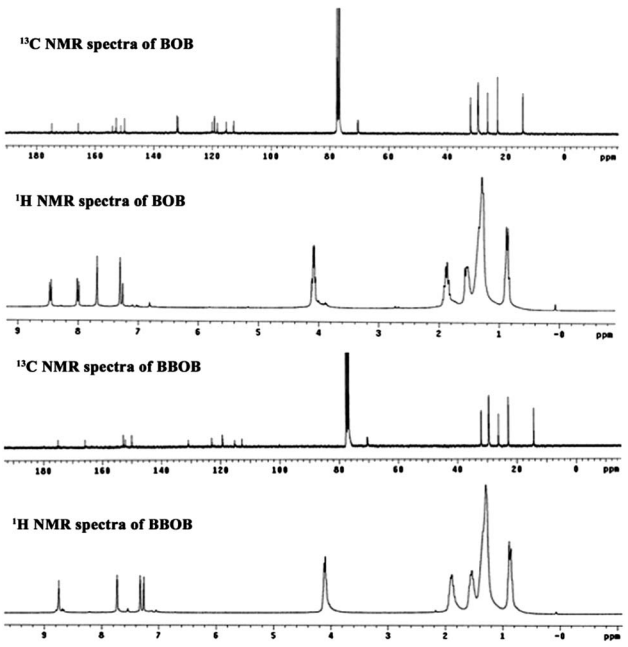

Fig. 2 The ^{1}H and ^{13}C NMR spectra of BBOB and BOB.

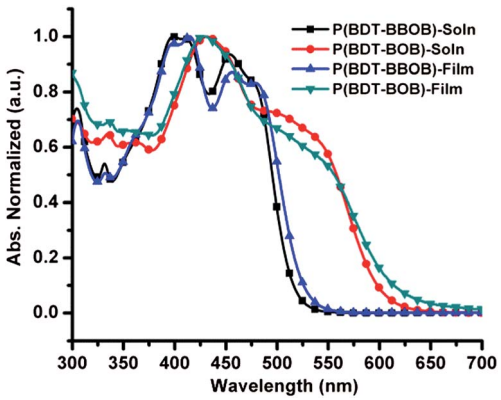

Fig. 3 Absorption spectra of polymers P(BDT-BBOB) and P(BDT-BOB) in chloroform and as a thin film.

both in solution and as a film. The absorption bands of **P(BDT-BBOB)** are expected to originate from the π–π transition, while those of **P(BDT-BOB)** might originate from the combined electronic transitions, such as by π–π transitions and donor–acceptor internal charge transfer (ICT) transitions between **BDT** and BT units. The presence of electron accepting Oxa units on both sides of the BT unit of **P(BDT-BBOB)** might restrict the ICT, but the covalent bond between the strong electron donating

Table 1 Polymerization results and thermal, optical, and electrochemical properties of P(BDT-BBOB) and P(BDT-BOB)

Polymer	M_w[a] (g mol^{-1})	PDI[a]	TGA[b] (°C)	λ_{max} in solution (nm)[c]	λ_{max} as film (nm)[d]	$E_{g,opt}$ (eV)[e]	HOMO (eV)[f]	LUMO (eV)[f]	$E_{g,elect}$ (eV)[g]
P(BDT-BBOB)	1.85×10^4	1.45	407	399, 454	416, 455	2.32	−5.31	−2.90	2.41
P(BDT-BOB)	2.13×10^4	1.63	415	431, 509	431, 509	1.99	−5.27	−3.10	2.17

[a] Weight average molecular weight (M_w) and polydispersities (PDI) of the polymers were determined by GPC using polystyrene standards. [b] 5% weight loss temperature measured by TGA under N_2. [c] Measurements in chloroform solution. [d] Measurements in thin film were performed on the glass substrate. [e] Band gap estimated from the onset wavelength of the optical absorption in thin film. [f] The HOMO and LUMO levels were estimated from cyclic voltammetry analysis. [g] The electrochemical band gap values estimated from the HOMO and LUMO values.

 This journal is © The Royal Society of Chemistry 2014

Published on 21 August 2014. Downloaded by University of Western Ontario on 28/10/2014 14:34:46.

BDT and electron accepting BT units of **P(BDT-BOB)** might allow the ICT. Earlier reports confirmed that the incorporation of sterically hindered electron donor groups, such as 3-octylthiophene or alkoxy benzene, or an electron accepting benzimidazole derivative on both sides of the BT restrict the ICT from the donor to the acceptor units when they are polymerized with electron-rich units.[15,17,23,34] These results suggest that the incorporation of Oxa units on both sides of the BT unit also diminish the ICT between the D–A units. The absorption onset wavelengths of **P(BDT-BBOB)** and **P(BDT-BOB)** were calculated to be 534 nm and 622 nm, respectively, from which the optical band gaps ($E_{g,opt}$) were determined to be 2.32 eV and 1.99 eV, respectively. The optical properties of polymers **P(BDT-BBOB)** and **P(BDT-BOB)** are summarized in Table 1.

3.3 Electrochemical properties

The highest occupied molecular orbital (HOMO) and lowest unoccupied molecular orbital (LUMO) energy levels of **P(BDT-BBOB)** and **P(BDT-BOB)** were estimated from cyclic voltammetry (CV) analysis, and the CV spectra of polymers are displayed in Fig. 4. The HOMO and LUMO energy levels of **P(BDT-BBOB)** and **P(BDT-BOB)** were calculated from the onset oxidation (E_{ox}) and onset reduction (E_{red}) potential values, by using the following equations, $E_{HOMO} = [-(E_{ox,onset\ vs.\ Ag/AgCl} - E_{ferrocene\ vs.\ Ag/AgCl}) - 4.8]$ eV and $E_{LUMO} = [-(E_{red,onset\ vs.\ Ag/AgCl} - E_{ferrocene\ vs.\ Ag/AgCl}) - 4.8]$ eV. The $E_{ferrocene\ vs.\ Ag/AgCl}$ is calculated from the oxidation potential of ferrocene standard to be 0.55 V. The $E_{ox,onset\ vs.\ Ag/AgCl}$ and $E_{red,onset\ vs.\ Ag/AgCl}$ values of **P(BDT-BBOB)** and **P(BDT-BOB)** were determined to be 1.06 V, 1.02 V and 1.35 V, 1.15 V, respectively. The HOMO/LUMO energy levels of **P(BDT-BBOB)** and **P(BDT-BOB)** were calculated to be −5.31 eV/−2.90 eV and −5.27 eV/−3.10 eV, respectively. The electrochemical band gap values were 2.41 eV and 2.17 eV, respectively. The electrochemical band gap ($E_{g,elect}$) values are found to be slightly higher than that of the optical band gap values ($E_{g,opt}$). The deeper HOMO energy levels of **P(BDT-BBOB)** and **P(BDT-BOB)**, and most importantly, the significant energy difference between the LUMO levels of newly synthesized polymers and $PC_{61}BM$ ensure that the polymers are suitable electron donors for PSCs application. The HOMO and LUMO energy levels of polymers **P(BDT-BBOB)** and **P(BDT-BOB)** are included in Table 1.

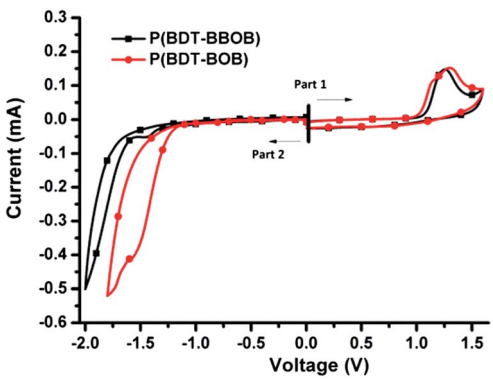

Fig. 4 Cyclic voltammograms of polymers P(BDT-BBOB) and P(BDT-BOB) films cast on a platinum working electrode in 0.1 M TBATFB/acetonitrile at 100 mV s^{-1}, potential *vs.* Fe/Fe^{+}.

3.4 Photovoltaic properties

The PSCs were fabricated with the device structure of ITO/PEDOT:PSS/**P(BDT-BBOB)** or **P(BDT-BOB)**:$PC_{61}BM$/LiF/Al. Among the devices prepared with three different donor:acceptor ratios of 1 : 1 wt%, 1 : 2 wt%, and 1 : 3 wt% for each polymer **P(BDT-BBOB)** or **P(BDT-BOB)** as a donor and $PC_{61}BM$ as an acceptor, the highest power conversion efficiency (PCE) was obtained for the devices made from 1 : 2 wt% blends. The current density–voltage (*J–V*) curves of the PSCs were measured under the illumination of AM 1.5 G (100 mW cm^{-2}), and their corresponding *J–V* curves are shown in Fig. 5. The characteristic parameters of the *J–V* curves of PSCs, such as open circuit voltage (V_{oc}), short-circuit current density (J_{sc}), fill factor (*FF*), and power conversion efficiency (PCE) are presented in Table 2. The device made from the blends of **P(BDT-BBOB)**:$PC_{61}BM$ (1 : 2 wt%) and **(BDT-BOB)**:$PC_{61}BM$ (1 : 2 wt%) gave an overall PCE of 1.76% (V_{oc} of 0.69 V, a J_{sc} of 7.10 mA cm^{-2}, and a FF of 36%) and 2.46% (V_{oc} of 0.71 V, a J_{sc} of 8.21 mA cm^{-2}, and a FF of 43%), respectively. Recently post-solvent treatment on the photoactive layer of the PSCs was reported to improve the photoactive performances of the PSCs significantly.[35–37] We also tried post-solvent treatment with various solvents, such as acetone, methanol, ethanol, and isopropyl alcohol (IPA), and the best result was obtained with IPA treatment. The PCE of the PSCs prepared from the blends of **P(BDT-BBOB)**:$PC_{61}BM$ (1 : 2

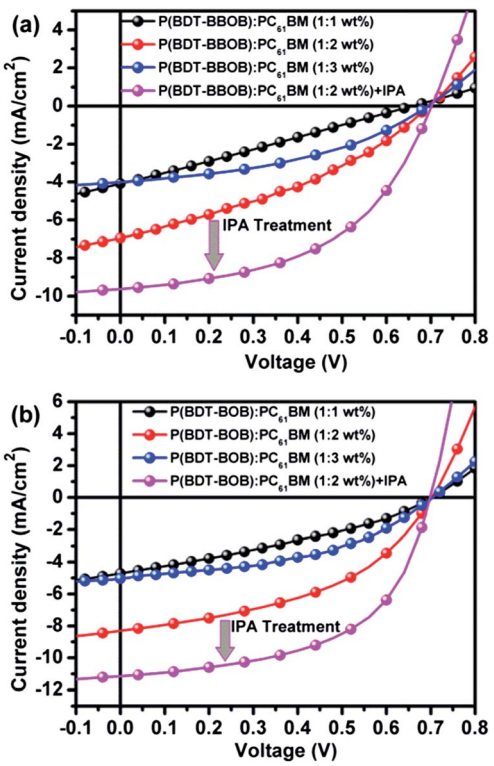

Fig. 5 *J–V* characteristics of PSCs prepared with the device structure of ITO/PEDOT:PSS/P(BDT-BBOB) or P(BDT-BOB):$PC_{61}BM$/LiF/Al.

Published on 21 August 2014. Downloaded by University of Western Ontario on 28/10/2014 14:34:46.

Table 2 PSCs performance of polymers P(BDT-BBOB) and P(BDT-BOB)

Polymer:$PC_{61}BM$ ratio	V_{oc} (V)[a]	J_{sc} (mA cm^{-2})[b]	FF (%)[c]	PCE (%)[d]	R_s (Ω cm^2)[e]	Integrated J_{sc} (mA cm^{-2})[f]
P(BDT-BBOB):$PC_{61}BM$ (1 : 1 wt%)	0.67 ± 0.02	4.09 ± 0.16	25.96 ± 0.01	0.72 ± 0.10	36	3.96 ± 0.12
P(BDT-BBOB):$PC_{61}BM$ (1 : 2 wt%)	0.69 ± 0.02	7.10 ± 0.18	35.75 ± 0.35	1.76 ± 0.10	15	7.03 ± 0.10
P(BDT-BBOB):$PC_{61}BM$ (1 : 3 wt%)	0.69 ± 0.01	3.96 ± 0.01	41.77 ± 0.01	1.15 ± 0.02	20	3.77 ± 0.10
P(BDT-BBOB):$PC_{61}BM$ (1 : 2 wt%) + IPA	0.70 ± 0.01	9.59 ± 0.28	49.43 ± 0.01	3.31 ± 0.08	10	9.57 ± 0.16
P(BDT-BOB):$PC_{61}BM$ (1 : 1 wt%)	0.70 ± 0.01	4.44 ± 0.26	33.33 ± 0.02	1.04 ± 0.03	31	4.31 ± 0.17
P(BDT-BOB):$PC_{61}BM$ (1 : 2 wt%)	0.71 ± 0.03	8.21 ± 0.09	42.60 ± 0.03	2.46 ± 0.16	12	8.10 ± 0.02
P(BDT-BOB):$PC_{61}BM$ (1 : 3 wt%)	0.70 ± 0.01	5.07 ± 0.05	45.43 ± 0.02	1.62 ± 0.05	14	5.00 ± 0.10
P(BDT-BOB):$PC_{61}BM$ (1 : 2 wt%) + IPA	0.70 ± 0.01	11.23 ± 0.16	53.82 ± 0.01	4.21 ± 0.10	6	11.07 ± 0.06

[a] Open-circuit voltage. [b] Short-circuit current density. [c] Fill factor. [d] Power conversion efficiency (averages of 5 PSC devices are reported for each blend). [e] Series resistance. [f] Estimated from IPCE curves.

wt%) and **(BDT-BOB)**:$PC_{61}BM$ (1 : 2 wt%) was further improved to 3.31% (V_{oc} of 0.70 V, a J_{sc} of 9.59 mA cm^{-2}, and a FF of 49%) and 4.21% (V_{oc} of 0.70 V, a J_{sc} of 11.23 mA cm^{-2}, and a FF of 54%), respectively, with IPA treatment on the active layer of PSCs.

The comparison of the device performances of **P(BDT-BBOB)** and **P(BDT-BOB)** suggests that the difference in the PCE mainly originates from their different J_{sc} and FF values. Usually, the J_{sc} and FF of the PSCs are affected by the absorption ability, series resistance (R_s), charge-transport properties, charge extraction, and charge recombination.[36] Polymer **P(BDT-BOB)** displayed a broad and red-shifted absorption band compared to polymer **P(BDT-BBOB)**, and consequently, the PSCs made from **P(BDT-BOB)** gave higher J_{sc} values than the PSCs made from **P(BDT-BBOB)**. The lower FF value obtained for **P(BDT-BBOB)** indicates that the presence of the additional Oxa unit on the polymer main chain might reduce their hole mobility, because oxadiazoles have a tendency to facilitate electron transport more effectively than the hole transport,[38–40] and consequently, it offered lower FF values compared with those of **P(BDT-BOB)**. The higher series resistance (R_s) values (measured from the dark J–V curves) of the PSCs made from **P(BDT-BBOB)**:$PC_{61}BM$ blends compared to those of the PSCs made from **P(BDT-BOB)**:$PC_{61}BM$ (1 : 2 wt%) agree with our arguments. In both cases, the series resistances of the PSCs were dramatically decreased after IPA treatment, as shown in Table 2, and consequently, higher J_{sc} and FF were obtained with IPA treatment.

To make clearer our argument, we estimated the hole mobility of each polymer and of the polymer:$PC_{61}BM$ blends by the space charge limited current (SCLC) method. The device structure used in this study and the corresponding SCLC characteristics for the hole-only devices made with the polymer or polymer:$PC_{61}BM$ blend as active layers are presented in Fig. 6. The device made with **P(BDT-BBOB)** and the **P(BDT-BBOB)**:$PC_{61}BM$ blend displayed relatively lower hole mobility, $\mu \sim 6.11 \times 10^{-5}$ cm^2 V^{-1} s^{-1} and 9.61×10^{-6} cm^2 V^{-1} s^{-1}, compared with that of the corresponding device made with the **P(BDT-BOB)** and **P(BDT-BOB)**:$PC_{61}BM$ blend ($\mu \sim 3.31 \times 10^{-44}$ cm^2 V^{-1} s^{-1} and 4.27×10^{-5} cm^2 V^{-1} s^{-1}, respectively). The higher hole mobility obtained for the **P(BDT-BOB)**-based device

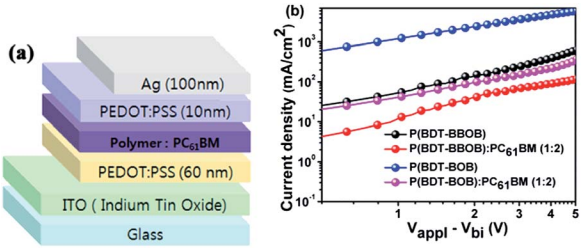

Fig. 6 (a) Schematic diagram of the hole-only device. (b) Current density–voltage (J–V) characteristics of the hole-only devices.

strongly supports the higher FF and J_{sc} obtained for the **P(BDT-BOB)**-based PSCs.

In order to investigate the effect of solvent treatment on the interface resistance of the PSCs, the electrochemical impedance spectra (EIS) of the PSCs were measured in the dark. Fig. 7 shows the Nyquist plots of the ac impedance of the PSCs based on **P(BDT-BBOB)** and **P(BDT-BOB)** without and with solvent treatment at 0 V with a frequency range from 1 Hz to 1 MHz. The ac impedance consists of a single depressed semicircle for each PSC, which can be used to calculate the internal resistance of the thin film for the PSC. For example, the equivalent resistance of the PSC made from **P(BDT-BBOB)** with solvent treatment is about 2086 Ω, which is much smaller than the value of about 3886 Ω for the PSC without solvent treatment (see Fig. 6a). This indicates that the solvent treatment layer can improve the contact between the photoactive layer and the top Al electrode and, consequently, decreases the resistance of the whole device. It is worth noting that the resistance of **P(BDT-BOB)**-based PSCs

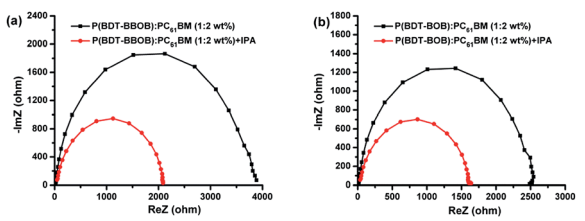

Fig. 7 Electrochemical impedance spectra of PSCs made from P(BDT-BBOB):$PC_{61}BM$ (1 : 2 wt%) and P(BDT-BOB):$PC_{61}BM$ (1 : 2 wt%) blends with/without IPA treatment.

 This journal is © The Royal Society of Chemistry 2014

Published on 21 August 2014. Downloaded by University of Western Ontario on 28/10/2014 14:34:46.

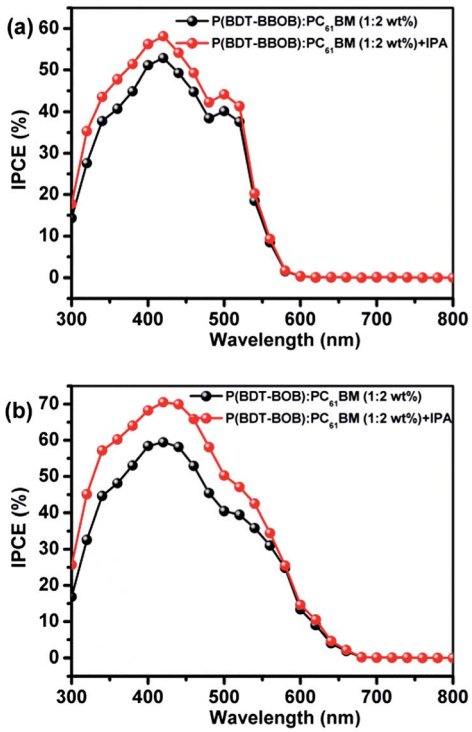

Fig. 8 IPCE spectra of the PSCs made from **P(BDT-BBOB)**:$PC_{61}BM$ (1 : 2 wt%) and **P(BDT-BOB)**:$PC_{61}BM$ (1 : 2 wt%) blends with/without IPA treatment.

are lower than that of **P(BDT-BBOB)**-based PSCs, which also supports our earlier arguments regarding the higher FF values obtained for **P(BDT-BOB)**-based PSCs.

The IPCE spectra of the PSCs made from **P(BDT-BBOB)**:$PC_{61}BM$ (1 : 2 wt%) and **P(BDT-BOB)**:$PC_{61}BM$ (1 : 2 wt%) blends with and without IPA treatment are displayed in Fig. 8. The IPCE responses were found to cover the region of 300–580 nm and 300–650 nm, respectively, for the PSCs made from **P(BDT-BBOB)** and **P(BDT-BOB)**. The maximum IPCE values at 420 nm appeared to be 53% and 58%, respectively, for the PSCs made from **P(BDT-BBOB)** without and with IPA treatment. On the other hand, the PSCs made from **P(BDT-BOB)** without and with IPA treatment showed the IPCE maximum values of 60% and 70%, respectively, at 420 nm. In both cases, the IPCE responses of the PSCs significantly increased after IPA treatment. These results strongly agree with the higher J_{sc} values obtained for the PSCs made with IPA treatment and also support the higher J_{sc} values obtained for the PSCs made from **P(BDT-BOB)**, compared with those obtained for the PSCs made from **P(BDT-BBOB)**. The integrated J_{sc} value of the PSCs determined from the IPCE spectra and the J_{sc} values obtained from the *J–V* curve of the PSCs are found to be within a 5% error range, and the integrated J_{sc} values are summarized in Table 2 for clear comparison.

3.5 Active layer surface morphology

The tapping mode atomic force microscopy (AFM) images of the films made from **P(BDT-BBOB)**:$PC_{61}BM$ (1 : 2 wt%) and **P(BDT-BOB)**:$PC_{61}BM$ (1 : 2 wt%) without and with IPA

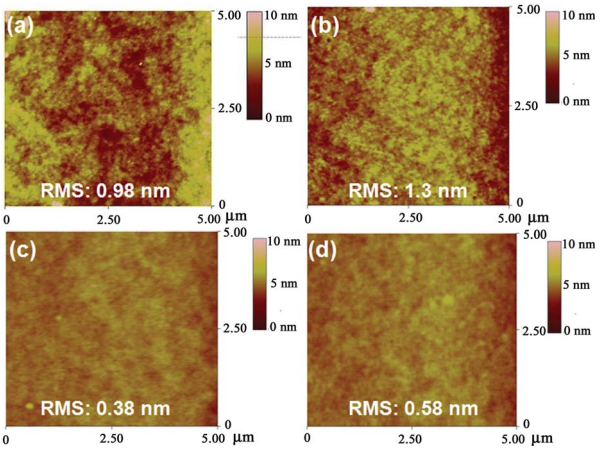

Fig. 9 AFM images of the blend films of **P(BDT-BBOB)**:$PC_{61}BM$ (1 : 2 wt%) and **P(BDT-BOB)**:$PC_{61}BM$ (1 : 2 wt%) without (images a and c, respectively) and with solvent treatment (images b and d, respectively).

treatment were recorded, as shown in Fig. 9. The rms roughness of the films made from **P(BDT-BBOB)**:$PC_{61}BM$ (1 : 2 wt%) and **P(BDT-BOB)**:$PC_{61}BM$ (1 : 2 wt%) increased from 0.98 nm to 1.3 nm, and from 0.38 nm to 0.58 nm, respectively, after applying the solvent treatment. The rough surface increases the contact area between the photoactive layer and the Al cathode, which may benefit a more efficient charge collection at the interface.[41] Moreover, the increased surface roughness may also increase the internal reflection and light collection, increasing the PSCs' efficiency.[42]

4. Conclusions

Two new electron accepting monomers (**BBOB** and **BOB**) containing two serially connected different electron deficient units, such as 2,1,3-benzothiadiazole (BT) and 1,2,4-oxadiazole (Oxa), were prepared and copolymerized with an electron-rich distannyl derivative of 4,8-bis(2-ethylhexyloxy)benzo[1,2-*b*:4,5-*b*′]-dithiophene (**BDT**) to afford polymers **P(BDT-BBOB)** and **P(BDT-BOB)**, respectively. Polymer **P(BDT-BBOB)** incorporating two Oxa units on both sides of the BT unit was found to show a blue-shifted absorption with a slightly lower HOMO level compared to those of polymer **P(BDT-BOB)** incorporating one Oxa unit attached to the BT unit. The maximum PCEs obtained for the PSCs made with the configuration of ITO/PEDOT:PSS/**P(BDT-BBOB)** or **P(BDT-BOB)**:$PC_{61}BM$ (1 : 2 wt%)/IPA/LiF/Al were 3.31% and 4.21%, respectively, measured using an AM 1.5 G solar simulator at 100 mW cm^{-2} light illumination. The presence of the additional Oxa unit on the polymer main chain was found to decrease the FF and J_{sc} values significantly and consequently, gave a lower PCE. This study concludes that the ratio or configuration of two covalently bonded different electron acceptor units present in the polymer main notably alters the optical, electrical, and photovoltaic properties of the polymers. We hope that replacement of the Oxa unit in polymer **P(BDT-BOB)** with other electron accepting units, such as thiadiazole, tetrazine, or thiazole, might enhance the PCE further, and currently progress is underway in this regard.

Published on 21 August 2014. Downloaded by University of Western Ontario on 28/10/2014 14:34:46.

Acknowledgements

This research was supported by the National Research Foundation of Korea (NRF-2013R1A2A2A04014576). This study was also supported by the research fund (PKC 3670) of Korea Institute of Materials Science.

Notes and references

1 R. Sondergaard, M. Hosel, D. Angmo, T. T. Larsen-Olsen and F. C. Krebs, *Mater. Today*, 2012, **15**, 36–49.
2 C.-C. Chen, L. Dou, J. Gao, W.-H. Chang, G. Li and Y. Yang, *Energy Environ. Sci.*, 2013, **6**, 2714–2720.
3 S. Esiner, H. V. Eersel, M. M. Wienk and R. A. J. Janssen, *Adv. Mater.*, 2013, **25**, 2932–2936.
4 W. Li, A. Furlan, K. H. Hendriks, M. M. Wienk and R. A. J. Janssen, *J. Am. Chem. Soc.*, 2013, **135**, 5529–5532.
5 K. Li, Z. Li, K. Feng, X. Xu, L. Wang and Q. Peng, *J. Am. Chem. Soc.*, 2013, **135**, 13549–13557.
6 J. You, L. Dou, K. Yoshimura, T. Kato, K Ohya, T. Moriarty, K. Emery, C.-C. Chen, J. Gao, G. Li and Y. Yang, *Nat. Commun.*, 2013, **4**, 1446–1510.
7 L. Dou, J. You, J. Yang, C.-C. Chen, Y. He, S. Murase, T. Moriarty, K. Emery, G. Li and Y. Yang, *Nat. Photonics*, 2012, **6**, 180–185.
8 G. Dennler, M. C. Scharber and C. J. Brabec, *Adv. Mater.*, 2009, **21**, 1323–1338.
9 N. Wang, Z. Chen, W. Wei and Z. Jiang, *J. Am. Chem. Soc.*, 2013, **135**, 17060–17068.
10 Z. He, C. Zhong, S. Su, M. Xu, H. Wu and Y. Cao, *Nat. Photonics*, 2012, **6**, 591–595.
11 C. Cabanetos, A. E. Labban, J. A. Bartelt, J. D. Douglas, W. R. Mateker, J. M. J. Frechet, M. D. McGehee and P. M. Beaujuge, *J. Am. Chem. Soc.*, 2013, **135**, 4656–4659.
12 L. Dou, W.-H. Chang, J. Gao, C.-C. Chen, J. You and Y. Yang, *Adv. Mater.*, 2013, **25**, 825–831.
13 L. Dou, J. Gao, E. Richard, J. You, C.-C. Chen, K. C. Cha, Y. He, G. Li and Y. Yang, *J. Am. Chem. Soc.*, 2012, **134**, 10071–10079.
14 R. R. Lunt, T. P. Osedach, P. R. Brown, J. A. Rowehl and V. Bulovic, *Adv. Mater.*, 2011, **23**, 5712–5727.
15 S. Wen, J. Pei, Y. Zhou, P. Li, L. Xue, Y. Li, B. Xu and W. Tian, *Macromolecules*, 2009, **42**, 4977–4984.
16 E. Zhou, S. Yamakawa, Y. Zhang, K. Tajima, C. Yanga and K. Hashimoto, *J. Mater. Chem.*, 2009, **19**, 7730–7737.
17 V. Tamilavan, M. Song, S.-H. Jin and M. H. Hyun, *Polymer*, 2011, **52**, 2384–2390.
18 H. Li, H. Luo, Z. Cao, Z. Gu, P. Shen, B. Zhao, H. Chen, G. Yub and S. Tan, *J. Mater. Chem.*, 2012, **22**, 22913–22921.
19 X. Guo, M. Zhang, L. Huo, F. Xu, Y. Wu and J. Hou, *J. Mater. Chem.*, 2012, **22**, 21024–21031.
20 L. Fan, R. Cui, X. Guo, D. Qian, B. Qiu, J. Yuan, Y. Li, W. Huang, J. Yang, W. Liu, X. Xu, L. Li and Y. Zou, *J. Mater. Chem. C*, 2014, **2**, 5651–5659.
21 X. Wang, S. Chen, Y. Sun, M. Zhang, Y. Li, X. Li and H. Wang, *Polym. Chem.*, 2011, **2**, 2872–2887.
22 Y. Cao, T. Lei, J. Yuan, J.-Y. Wang and J. Pei, *Polym. Chem.*, 2013, **4**, 5228–5236.
23 V. Tamilavan, M. Song, R. Agneeswari, S. Kim and M. H. Hyun, *Bull. Korean Chem. Soc.*, 2014, **35**, 1098–1104.
24 V. Tamilavan, M. Song, S.-H. Jin and M. H. Hyun, *Synth. Met.*, 2011, **161**, 1199–1206.
25 V. Tamilavan, M. Song, S.-H. Jin, H. J. Park, U. C. Yoon and M. H. Hyun, *Synth. Met.*, 2012, **162**, 1184–1189.
26 M. L. Keshtov, D. V. Marochkin, V. S. Kochurov, A. R. Khokhlov, E. N. Koukarascd and G. D. Sharma, *J. Mater. Chem. A*, 2014, **2**, 155–171.
27 L. Wang, D. Cai, Q. Zheng, C. Tang, S.-C. Chen and Z. Yin, *ACS Macro Lett.*, 2013, **2**, 605–608.
28 G. Li, C. Kang, X. Gong, J. Zhang, W. Li, C. Li, H. Dong, W. Hub and Z. Bo, *J. Mater. Chem. C*, 2014, **2**, 5116–5123.
29 R. Agneeswari, V. Tamilavan, M. Song, J.-W. Kang, S.-H. Jin and M. H. Hyun, *J. Polym. Sci., Part A: Polym. Chem.*, 2013, **51**, 2131–2141.
30 S. Lightowler and M. Hird, *Chem. Mater.*, 2004, **16**, 3963–3971.
31 M. Jorgensen and F. C. Krebs, *J. Org. Chem.*, 2005, **70**, 6004–6017.
32 J. U. Ju, S. O. Jung, Q. H. Zhao, Y. H. Kim, J. T. Je and S. K. Kwon, *Bull. Korean Chem. Soc.*, 2008, **29**, 335–338.
33 L.-Y. Lin, C.-W. Lu, W.-C. Huang, Y.-H. Chen, H.-W. Lin and K.-T. Wong, *Org. Lett.*, 2011, **13**, 4962–4965.
34 V. Tamilavan, M. Song, S. Kim, R. Agneeswari, J.-W. Kang and M. H. Hyun, *Polymer*, 2013, **54**, 3198–3205.
35 Y. Wang, Y. Liu, S. Chen, R. Peng and Z. Ge, *Chem. Mater.*, 2013, **25**, 3196–3204.
36 H. Zhou, Y. Zhang, J. Seifter, S. D. Collins, C. Luo, G. C. Bazan, T.-Q. Nguyen and A. J. Heeger, *Adv. Mater.*, 2013, **25**, 1646–1652.
37 H. Li, H. Tang, L. Li, W. Xu, X. Zhao and X. Yang, *J. Mater. Chem.*, 2011, **21**, 6563–6568.
38 E. Hamciuc, C. Hamciuc and M. Cazacu, *Eur. Polym. J.*, 2007, **43**, 4739–4749.
39 P. D. Vellis, J. A. Mikroyannidis, M. J. Cho and D. H. Choi, *J. Polym. Sci., Part A: Polym. Chem.*, 2008, **46**, 5592–5603.
40 F. Dumur and F. Goubar, *New J. Chem.*, 2014, **38**, 2204–2224.
41 G. Li, V. Shrotriya, Y. Yao and Y. Yang, *J. Appl. Phys.*, 2005, **98**, 043704.
42 H.-Y. Lee and H.-L. Huang, *Int. J. Photoenergy*, 2014, **2014**, 812643.

 This journal is © The Royal Society of Chemistry 2014